# GEOMETRIC GRAPHS FROM DATA TO AID CLASSIFICATION TASKS WITH GRAPH CONVOLUTIONAL NETWORKS

#### Yifan Qian

School of Business and Management Queen Mary University of London London, UK y.qian@qmul.ac.uk

# Pietro Panzarasa

School of Business and Management Queen Mary University of London London, UK p.panzarasa@gmul.ac.uk

#### Paul Expert

School of Public Health Imperial College London London, UK paul.expert08@imperial.ac.uk

#### Mauricio Barahona

Department of Mathematics Imperial College London London, UK m.barahona@imperial.ac.uk

## **ABSTRACT**

Classification is a classic problem in data analytics and has been approached from many different angles, including machine learning. Traditionally, machine learning methods classify samples based solely on their features. This paradigm is evolving. Recent developments on Graph Convolutional Networks have shown that explicitly using information not directly present in the features to represent a type of relationship between samples can improve the classification performance by a significant margin. However, graphs are not often immediately present in data sets, thus limiting the applicability of Graph Convolutional Networks. In this paper, we explore if graphs extracted from the features themselves can aid classification performance. First, we show that constructing optimal geometric graphs directly from data features can aid classification tasks on both synthetic and real-world data sets from different domains. Second, we introduce two metrics to characterize optimal graphs: i) by measuring the alignment between the subspaces spanned by the features convolved with the graph and the ground truth; and ii) ratio of class separation in the output activations of Graph Convolutional Networks: this shows that the optimal graph maximally separates classes. Finally, we find that sparsifying the optimal graph can potentially improve classification performance.

**Keywords** Classification tasks · Machine learning · Graph Convolutional Networks · Graph construction · Graph sparsification

#### Introduction

The classification of samples into a given number of classes is one of the fundamental tasks of data analytics [1]. In a supervised learning setting, *traditional* machine learning methods train a classifier using a training data set where both features and class labels are known for each observation. Once the classifier has learned from the training data, it can be used to predict the class of a new sample based on its features. Intuitively, a good classification for unseen samples can be obtained if the classifier can learn a representation of the data where samples belonging to different classes are well separated. To achieve the best possible separation, directly observed relational information between samples could be used as guiding lines for groups. Graphs are a natural way to represent such relational information, and a large number of machine learning methods can leverage the graph structure. Graph Neural Networks (GNNs) is a nascent class of such methods and refers to a fairly broad set of techniques attempting to extend deep neural models to graph-structured data [2]. GNN has witnessed success in a variety of research domains including computer vision [3, 4], natural language processing [5, 6, 7], traffic [8, 9], recommendation systems [10, 11], chemistry [12, 13] and many others [14, 15, 16, 17, 18, 19]. For a further review of GNN, we refer readers to [20]. Recently, the particular method

of Graph Convolutional Networks (GCNs) [5] has suggested that incorporating a graph structure between samples with their individual features information can improve the node, i.e., sample, classification performance compared with traditional methods using only features. The graph structure allows the definition of a convolution operation that passes and aggregates the features of samples that are connected. If the graph and the features capture well the underlying class structure and the latter is well separated, the convolution operation homogenizes features of neighboring nodes, while making less similar samples belong to other classes.

A necessary condition to apply GCN is to possess an explicit graph structure. However, in many cases, a graph structure is not directly observable. To address this limitation, we empirically explore the benefit of constructing geometric graphs from the features of the samples and using them with GCN for sample classification (Fig. 1a). Graph construction, or inference, is a problem encountered in many fields, from neuroimaging to genetics, and can be based on many different types of heuristics, from simple thresholding [21], statistically significant group level thresholding [22] to sophisticated regularization scheme [23]. The goal is always to obtain graphs that preserve desirable key properties of the original data set. In this work, we first examine several popular geometric graph construction methods and characterize the performance dependence on the graph density to find the optimal graph that maximally improves the classification performance. Among these methods, we show that the recently proposed Continuous *k*-Nearest Neighbor (CkNN) [24] performs well for GCN classification. Then, we propose two simple measures, alignment and ratio of class separation, to characterize the role of the constructed graphs in the classification. Finally, we show that sparser graphs obtained from the optimal CkNN graphs via spectral graph sparsification [25] can further improve, or at least give comparable, classification performance.

# Geometric graphs constructed from data features can aid classification

We have considered two families of graph construction methods: (i) neighborhood-based methods: k-Nearest Neighbor (kNN), Mixed k-Nearest Neighbor (MkNN) and Continuous k-Nearest Neighbor (CkNN) [24]; and (ii) a method based on Minimum Spanning Tree (MST): the Relaxed Minimum Spanning Tree (RMST) [26]. See Section Materials and Methods for a full description of those methods. For each of those graph construction methods, a parameter regulates the density of edges: k in kNN, MkNN and CkNN, and  $\gamma$  in RMST. Note that for neighborhood-based methods, an MST graph is added to ensure that the resulting graph always forms a single connected component. The optimal density parameter is selected based on the classification accuracy obtained for the validation set for each data set and each graph construction method. To this end, we systematically scan the density parameters to construct graphs such that their densities range approximately from 0 (very sparse) to 1 (very dense). Thus the two bounds approximately correspond to two limiting cases: no graph (density = 0), which corresponds to MLP, and the complete graph (density = 1), which corresponds to the mean field limit. We then run GCN with the constructed graphs and select the one with the highest mean accuracy on the validation set as the optimal graph (Fig. 1b). If the maximum value corresponds to multiple constructed graphs, we choose the sparsest one.

We have numerically investigated 7 data sets from very different domains, ranging from text (e.g., AMiner [27, 28]) to music track features (e.g., FMA [29, 30]) to single-cell transcriptomics (e.g., Cell [31]). Detailed description of data sets is provided in the SI Appendix. With optimal graphs as inputs to GCN, our experiments suggest that GCN are at least competitive and often achieve better results on classification problems compared to the graph-less baselines we considered: Multi-layer Perceptron (MLP), kNN classification (kNNC), Support Vector Machine (SVM) and Random Forest (RF) (Table 1c). In particular, we observe that the CkNN graph construction method achieves the highest accuracy improvement on the test set on average among the graph construction methods we considered.

# Why proper graphs can aid classification?

The graph construction method presented above can be seen as a *densification* process and we have shown that incorporating geometric graphs can improve classification performance provided they are well chosen. The graph densification procedure suggests that i) over-sparse graphs often do not help improve the classification where the performance is close to the no graph limiting case (MLP); ii) over-dense graphs are usually detrimental for classification, as the high density limit corresponds to the mean field limits, where the performance is significantly lower than no graph, and close to random guessing; and therefore iii) that optimal graphs usually sit at a sweet spot in terms of density. In this section, we will uncover the role of the constructed graphs at the optimal density and explore conditions indicative of optimality from two perspectives.

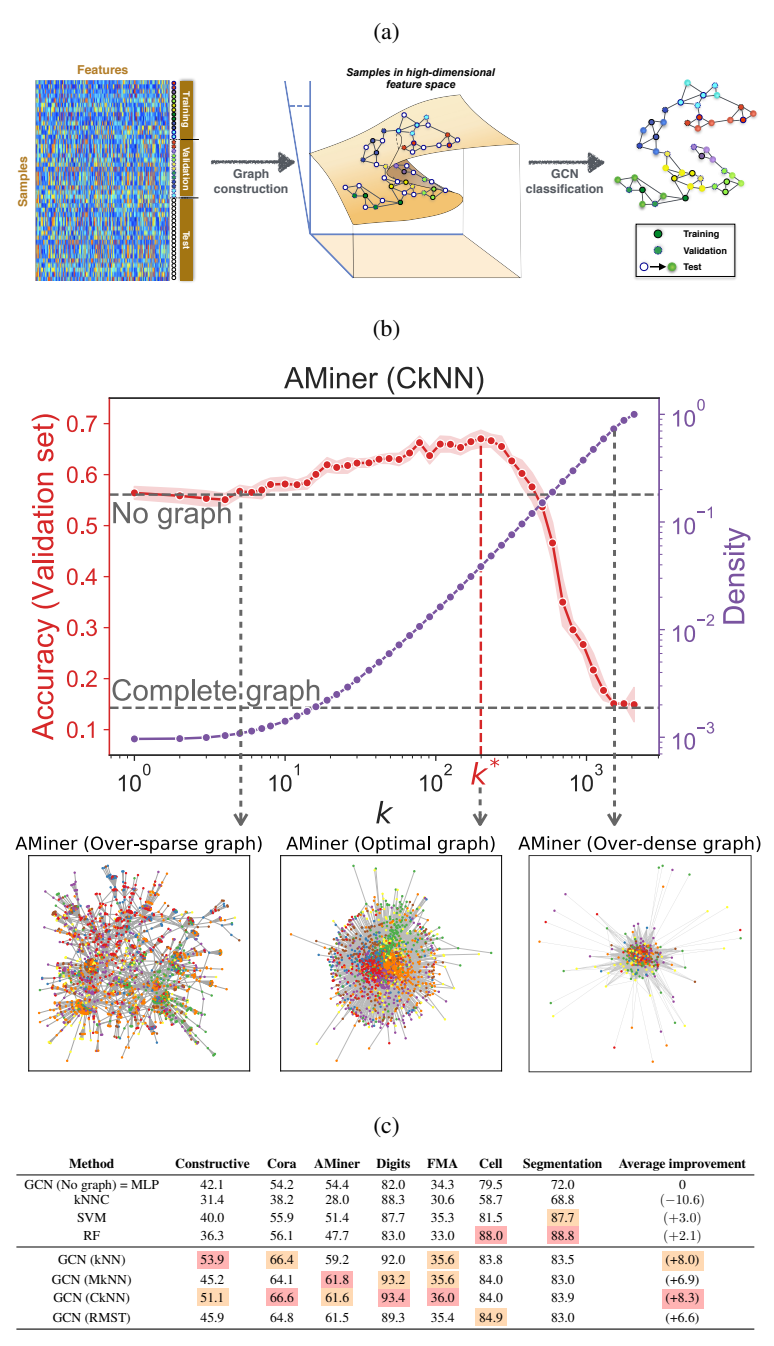


Figure 1: Panel (A): Schematic diagram of the workflow for classification using GCN with constructed graph. Panel (B): Optimal CkNN graph construction search process on AMiner. The red line indicates the mean classification accuracy on the validation set of 10 runs with random weight initializations as a function of the density parameter k in CkNN. The red shaded regions denote the standard deviation. The mean classification accuracy on the validation set of two limiting cases (no graph and complete graph) are added as well. The red vertical dashed line indicates the optimal graph. The graph visualizations with spring layout of an over-sparse graph, the optimal graph and an over-dense graph are also shown. The color of a node represents its corresponding ground truth class label. The purple line shows the densities of the constructed CkNN graphs. Results on other graph construction methods and data sets are provided in the SI Appendix. Panel (C): Summary of results in terms of mean classification accuracy (in percent) on the test set of 10 runs with random weight initializations. Results on density parameters of optimal graphs are provided in the SI Appendix.

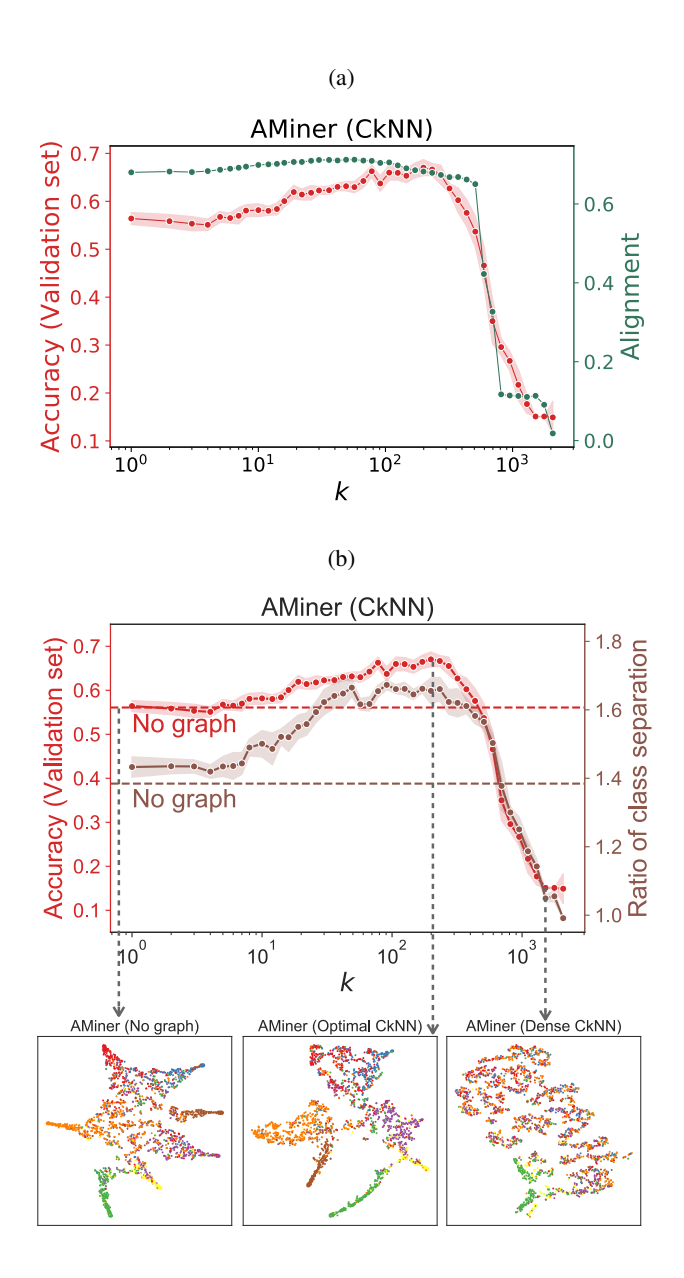


Figure 2: Panel (A): The red line indicates the mean classification accuracy on the validation set of 10 runs with random weight initializations as a function of the density parameter k in CkNN. The red shaded regions denote the standard deviation. The green line indicates the alignment according to Eq. 1. Results on other graph construction methods and data sets are provided in the SI Appendix. Panel (B): The red line indicates the mean classification accuracy on the validation set of 10 runs with random weight initializations as a function of the density parameter k in CkNN. The red shaded regions denote the standard deviation. The red dashed line represents the mean classification accuracy on the validation of no graph case. The brown line shows the ratio of class separation in the densification process. The brown shaded regions denote the standard deviation. The brown dashed line represents the ratio of class separation of no graph case. T-SNE visualizations of the output activations of GCN on the AMiner data set are also added for no graph, optimal graph and an over-dense graph. Each scatter represents a sample, and the color represents its ground truth label. Results on other graph construction methods and data sets are provided in the SI Appendix.

## Over-dense graphs degrade the subspace alignment of ingredients

Qian et al. [32] proposed that a certain degree of alignment among features  $X \in R^{N \times F}$ , graph  $\widehat{A} \in R^{N \times N}$  and ground truth  $Y \in R^{N \times C}$  is needed to obtain good performance of GCN (See Section Materials and Methods for a full description of GCN). N is the number of samples, F is the number of features of each sample and C is the number of classes in the data set. Inspired by the subspace alignment measure (SAM) proposed in [32], we compute the alignment  $S(X, \widehat{A}, Y)$  (Eq. 1) among the three ingredients as the cosine of *minimal* principal angle,  $\theta_1$ , between subspaces [33, 34, 35] associated with the convolved features  $\widehat{A}X$  and ground truth Y. The subspaces of convolved features and ground truth are spanned by the principal components of  $\widehat{A}X$  and Y obtained by Principal Component Analysis (PCA). The numbers of principal components are selected with the ratio of variance (0 explained.

$$S(X, \widehat{A}, Y) = \cos\left(\theta_1(\mathcal{X}, \mathcal{Y})\right) \tag{1}$$

where  $\mathcal{X}$  and  $\mathcal{Y}$  are corresponding column spaces of matrices  $PCA(\widehat{A}X, p)$  and PCA(Y, p), which are subspaces of the ambient space of  $\mathbb{R}^N$ .

We scan the ratio of explained variance in the range [0.1, 0.9] to maximize the Pearson correlation coefficient between alignment and mean classification accuracy on the validation set in the densification direction for each data set, respectively. Fig. 2a shows that the mean classification accuracy on the validation set is clearly correlated with the alignment between subspaces for AMiner. Similar figures for all data sets are in the SI Appendix. On average, the Pearson correlation coefficient on data sets is 0.852.

# Optimal graphs produce a large ratio of class separation

The matrix of output activations of GCN, i.e.,  $Z \in R^{N \times C}$  (see Eq. 9), is a row-stochastic membership assignment matrix with each row summing to 1. GCN assigns a sample to the class with the largest value in the corresponding row. The structure of the matrix Z is thus a representation of the classification performance and different constructed graphs will result in different Z for the same data set. Optimal graphs are expected to be able to separate well samples from different classes while making samples from the same classes clustered together in the C-dimensional space according to Z. We quantify the degree of class separation through the ratio between inter-class separation and intra-class separation based on the 2D embedding  $Z' \in R^{N \times 2}$  of Z using the t-distributed Stochastic Neighbor Embedding (t-SNE) [36] method. Specifically, we compute the average inter-class Euclidean distance from all pairs of samples from different classes and the average intra-class Euclidean distance from all pairs of samples from the same class, and use the ratio between the former and the latter as a measure of ratio of class separation (RCS) (Eq. 2). The RCS is formally defined as:

$$RCS = \frac{\left(\sum_{ij} (D^{(Z')} \circ M^{\text{inter}})\right) / \left(\sum_{ij} M^{\text{inter}}\right)}{\left(\sum_{ij} (D^{(Z')} \circ M^{\text{intra}})\right) / \left(\sum_{ij} M^{\text{intra}}\right)},\tag{2}$$

where  $D^{(Z')}$  is the Euclidean distance matrix associated with Z', i.e.,  $D^{(Z')}_{ij} = \left\| Z'_i - Z'_j \right\|_2$ .  $\circ$  represents Hadamard (element-wise) product between two matrices.  $M^{\text{inter}} \in R^{N \times N}$  is the inter-class indication matrix in which  $M^{\text{inter}}_{ij} = 1$  if samples i and j belong to different classes, and  $M^{\text{inter}}_{ij} = 0$  otherwise. Similarly,  $M^{\text{intra}} \in R^{N \times N}$  is defined as intra-class indication matrix. Formally,  $M^{\text{inter}}$  and  $M^{\text{inter}}$  can be efficiently computed by:

$$M^{\text{inter}} = \mathbf{1}\mathbf{1}^T - YY^T$$
  
 $M^{\text{intra}} = YY^T - I_N$ 

where  $I_N \in \mathbb{R}^{N \times N}$  is an identity matrix.

The RCS for AMiner with CkNN graphs in the densification direction is shown in Fig. 2b. Similar figures for all data sets are in the SI Appendix. We observe that there is a very high correlation between RCS and the mean classification performance on the validation set. The average Pearson correlation coefficient among data sets is 0.938. In particular, it is suggested that the optimal graphs maximize the RCS while over-dense graphs correspond to relatively smaller ratios. The RCS of extremely dense graphs is close to 1, which shows that, on average, inter-class and inter-class separation are not distinguishable, as all samples are convolved together.

# Graph sparsification improves classification performance while making the graph sparser

Sparse graph are generally favored over denser ones, in particular for large data sets, as they are cheaper to deal with for both numerical computation and data storage. We investigate whether it is possible to obtain a sparser representation of the optimal graph obtained from the CkNN densification process that preserve the spectral properties we think are important for improving the classification performance and therefore maintains a similar accuracy. To this end, we apply the well-known Spielman-Srivastava sparsification algorithm (SSSA) proposed in [25] to sparsify the optimal CkNN graphs. SSSA is a spectral sparsification method which aims at obtaining a spectral approximation of a given graph. The sparsification in SSSA is control by the parameter  $(\sigma)$  which can range from 0 to 1: the larger the value of  $\sigma$ , the sparser the resulting graph.

We scan  $\sigma$  for values ranging from 1/N to 1 for each data set, starting from the optimal CkNN graph obtained in the densification direction. We also choose optimal sparsified graphs based on the mean classification accuracy on the validation set (Fig. 3a). From an operational point of view, when deciding on the final optimal graph to be used, one has to balance between accuracy and computational efficiency as the mean classification accuracy on the test set of the optimal sparsified graph can be lower than no sparsification. Here, as we are purely concerned with accuracy, we choose the unsparsified graph, i.e.,  $\sigma=0$ . Our experiments suggest that graph sparsification can improve classification while making the graph sparser (Table 3b). We further replicate our experiments on the other top 3 CkNN graphs according to the mean classification accuracy on the validation set in the densification process, and results are consistent (See SI Appendix). We also find that there is a high correlation between classification performance on the validation set and RCS and alignment in the sparsification process, see the SI Appendix.

# **Discussion**

Our first set of experiments is centered around finding the optimal the graph that possess the maximal accuracy improvement and (Table 1c) shows that optimal CkNN graphs are a good choice for classification via GCN. This finding is in line with recent results on geometric graphs construction for clustering tasks [37]. CkNN graphs were proposed to offer a consistent discrete approximation of the diffusion operator on the manifold underlying the graph. Since GCN uses the graph to guide the nodes (i.e., samples) to diffuse features to neighboring nodes, this offers a natural explanation for the good performance of CkNN for classification tasks with GCN. RMST graphs also perform well, but not to the level of CkNN graphs. We conjecture that is due to the non-local similarities captured by RMST graphs. While they do not outperform neighborhood-based methods in the examples presented here, RMST graphs are able to capture relationships that are based on the existence of longer paths, which could be important for clusters that are not 'Gaussian', i.e., the similarity distribution is not monotonously decreasing with distance.

We expect geometric graphs to be most useful when data features are high-dimensional and noisy. All of the data sets (except Segmentation) in our experiments are high-dimensional. On these data sets, GCN with optimal graphs significantly outperforms the graph-less methods. In contrast, Segmentation has 19 engineered features that have already been optimized for classification. This is precisely the case where SVM and RF would work well. Nevertheless, we observe that even in these cases, the constructed graphs significantly improve the classification performance with respect to MLP, indicating that a well constructed graph is helping to filter out features similarities that can lure MLP.

To explore the reason behind the benefit of a geometric graph to the classification performance, inspired by [32], we proposed a simple subspace alignment measure (Eq. 1) that uses minimal principal angle to capture the congruence between the subspace of the features convolved by the constructed graphs and the ground truth. The proposed alignment correlates well with the classification performance. In particular, over-dense graphs greatly reduce the alignment in the densification process (Fig. 2a). The disadvantage of the over-dense graph is analogous to the over-smoothing problem for deeper layers of GCN that have been studied in [38, 39]. In addition, we computed the ratio of class separation (RCS) of the output activations of GCN and showed that optimal graphs can increase the separation between the samples of different classes (Fig. 2b). In contrast, over-sparse and over-dense graphs yield lower values of RCS, which explains intuitively the rapid decline in classification performance.

In addition, our numerics show that sparsifying the optimal CkNN graphs while preserving its spectral properties can improve the classification performance (Fig. 3). We choose SSSA since the spectral property of a graph associated with Laplacian quadratic form (Eq. 8) is related to the partition of a graph [40].

Besides having potential performance benefits, using a graph changes the classification paradigm from supervised learning (e.g., MLP) to semi-supervised learning (e.g., GCN) and therefore potentially from an inductive to a transductive learning paradigm. The supervised learning by definition belongs to the inductive class, while graph-based semi-supervised learning paradigms may refer to either transductive or inductive learning. GCN classification belongs to transductive learning. Thus using a graph, while potentially improving the classification performance, can also restricts

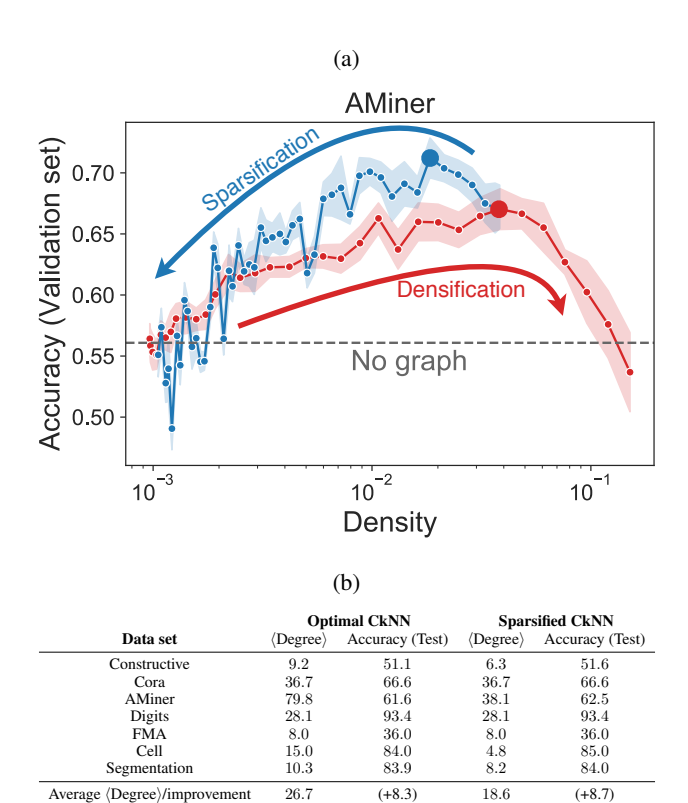


Figure 3: Panel (A): The red line indicates the mean classification accuracy on the validation set of 10 runs with random weight initializations as a function of the density. The red shaded regions denote the standard deviation. The bigger red dot represents the optimal graph in the densification process. Starting from the optimal graph, the blue line indicates the mean classification accuracy on the validation set of 10 runs with random weight initializations as a function of the density in the sparsification process. The blue shaded regions denote the standard deviation. The bigger blue dot represents the optimal graph in the sparsification process. The gray dashed line represents the mean classification accuracy on the validation of no graph case. Results on other data sets are provided in the SI Appendix. Panel (B): Comparison between optimal graphs from the densification process and sparsified graphs from the sparsification process. Average degree ( $\langle \text{Degree} \rangle$ ) in the graph and mean classification accuracy (in percent) on the test set of 10 runs with random weight initializations are reported. Average  $\langle \text{Degree} \rangle$  and average improvement of the accuracy on the test set compared with MLP are also added.

the generalizability of the model. While depending on the task considered it is not necessarily a problem, we believe it is possible to restore some generalizability: for a new sample that was not in the original data, one could first identify a few (e.g., the average degree of the optimal CkNN graph) closest samples in terms of Euclidean distance using original features, and then use the average values of rows in Z we stored of these neighbors to predict the class label of the new sample.

Our study opens several avenues for future work. Here we explored graph construction based on geometric property, it will be interesting to consider other graph construction paradigms by incorporating other criteria with geometry, e.g., small-world and graph expander. We showed that spectral sparsification [41] is a good choice to sparsify optimal graphs. However, other graph sparsification paradigms might also be useful, e.g., cut sparsification [42].

## Conclusion

Our empirical study on a number of data sets shows that constructing geometric graphs from features can aid classification tasks. The densification-sparsification graph construction framework we introduced can be combined with advanced graph-based deep learning methods and applied to a broad range of empirical domains.

## **Materials and Methods**

#### **Graph construction**

According to feature vectors  $X_i$  of samples, pairwise dissimilarity between them can be computed using a distance metric, e.g., Manhattan distance, Euclidean distance and many others. We consider a data set consisting of N samples. In this work, we choose Euclidean distance as the measure of dissimilarity. Specifically, for two samples i and j, Euclidean distance d(i,j) between them is defined as:

$$d(i,j) = \|X_i - X_j\|_2 \tag{3}$$

Based on the pairwise distance between samples, a graph can be constructed from very different heuristics. Here we mainly focus on two types of methods for graph construction: (i) methods based on the neighborhood: k-Nearest Neighbor (kNN), Mixed k-Nearest Neighbor (MkNN) and Continuous k-Nearest Neighbor (CkNN) [24]; and (ii) a method based on Minimum Spanning Tree (MST): Relaxed Minimum Spanning Tree (RMST) [26]. In this work, we consider constructing unweighted and undirected graphs. We always perform L1 normalization on the original features before constructing the graphs.

### Neighborhood-based methods

The objective of neighborhood-based methods is to construct a sparse graph by connecting two samples if they are local neighbors determined by their pairwise distance d(i,j). The simplest algorithm of this family is k-Nearest Neighbor (kNN). A kNN graph has an edge between two samples i and j if one of them belongs to the k-nearest neighbors of the other. Formally, the adjacency matrix  $A^{kNN} \in \mathbb{R}^{N \times N}$  of a kNN graph is defined as:

$$A_{i,j}^{\rm kNN} = \begin{cases} 1 & \text{if } d(i,j) \le d(i,i_k) \text{ or } d(i,j) \le d(j,j_k) \\ 0 & \text{otherwise} \end{cases} \tag{4}$$

where  $i_k$  and  $j_k$  represent the k-th nearest neighbors of samples i and j, respectively.

As one of the simplest and most widely used algorithms for graph construction, kNN has some limitations. One of the severe limitations is that kNN graphs can often produce hubs, i.e., samples with extremely high degree, since kNN greedily connects two samples as long as one of them belongs to the other's k-nearest neighbors. It has been suggested that, in graphs produced by kNN, the phenomenon that hubs emerge is particularly obvious when the features of samples are high-dimensional [43], and hubs tend to deteriorate the classification accuracy of semi-supervised learning [44]. To overcome this limitation, Mutual k-Nearest Neighbor (MkNN), a variant of kNN, has been proposed [44]. An MkNN graph is defined as a graph in which an edge is established between two samples i and j if each of them belongs to the other's k-nearest neighbors. Formally, the adjacency matrix  $A^{MkNN} \in \mathbb{R}^{N \times N}$  of an MkNN graph is defined as:

$$A_{i,j}^{\text{MkNN}} = \begin{cases} 1 & \text{if } d(i,j) \le d(i,i_k) \text{ and } d(i,j) \le d(j,j_k) \\ 0 & \text{otherwise} \end{cases}$$
 (5)

Note that MkNN algorithm can guarantee that the degrees of all samples are bounded by k. Therefore, MkNN is less likely to result in hubs compared with kNN especially when k is selected adequately small.

Another severe limitation is involved in the following process related to kNN. Note that a density parameter k needs to be predefined in the kNN algorithm. The choice of k is critical which can be an integer ranging from 1 to N-1. The larger the k, the denser the kNN graph. On the one hand, a very small value of k means that the noise potentially has a higher influence on the results. On the other hand, a very large value of k seems to violate the basic assumption of kNN that samples which are far away from each other probably belong to distinct classes. The parameter k is thus often selected based on the density of the data points. However, in many data sets, the sample points are not uniformly distributed [37]. Continuous k-Nearest Neighbor (CkNN) [24], a less discrete variant of kNN, has recently been introduced to address this limitation. The adjacency matrix  $A^{\text{CkNN}} \in \mathbb{R}^{N \times N}$  associated with a CkNN graph is defined as:

$$A_{i,j}^{\text{CkNN}} = \begin{cases} 1 & \text{if } d(i,j) < \delta \sqrt{d(i,i_k)d(j,j_k)} \\ 0 & \text{otherwise} \end{cases}$$
 (6)

where  $\delta$  is a positive parameter that regulates the density of the graph. The larger the  $\delta$ , the denser the CkNN graph for a fixed k. The authors of [24] have shown that the CkNN graph can capture the geometric features of the samples with the additional consistency that (unnormalized) Laplacian of the CkNN graph converges spectrally to a Laplace-Beltrami operator in the limit of large data. In this work, we fix  $\delta=1$  and vary different k such that CkNN can be compared with kNN and MkNN as suggested in [37].

#### MST-based methods

Neighborhood-based methods are designed to capture mainly the geometric information of local neighborhood. Conversely, a different family of graph construction methods attempts to retrieve the global geometry of all the samples in the data set by considering the measures of global connectivity. A standard and simple way to ensure the global connectivity is Minimum Spanning Tree (MST). The MST graph construction involves two steps: (i) constructing a distance matrix of all samples  $D \in R^{N \times N}$  where  $D_{i,j} = d(i,j)$ . D thus can be seen as the adjacency matrix of a fully connected graph where edge weights are distances between samples; and (ii) finding a subgraph (MST) of the fully connected graph corresponding to D such that all the samples are connected through one path and the sum of edge weights is minimized. We use  $A^{\rm MST}$  to represent the adjacency matrix of the constructed MST graph. Note that the number of edges of an MST graph of N nodes is N-1. to ensure the global connectivity, we always impose an MST graph on the constructed graph from neighborhood-based methods.

In recent years, several advanced algorithms have been introduced to explore global properties of MST by proposing MST-based graphs [37]. In this work, we focus on Relaxed Minimum Spanning Tree (RMST) [26]. RMST considers the largest edge weight  $d_{\text{MST-path}(i,j)}^{\text{max}}$  in D along the MST-path between i and j. If  $d_{\text{MST-path}(i,j)}^{\text{max}}$  is significantly smaller than d(i,j), RMST discards the direct link between i and j, i.e.,  $A_{i,j}^{\text{RMST}} = 0$ , since MST-path is considered as a good model to explain the similarity between them. However, if d(i,j) is comparable to  $d_{\text{MST-path}(i,j)}^{\text{max}}$ , there is no sufficient evidence that MST-path is a better model, and RMST adds the direct link  $A_{i,j}^{\text{RMST}} = 1$ . Specifically, RMST uses the following heuristic based on MST:

$$A_{i,j}^{\text{RMST}} = \begin{cases} 1 & \text{if } d(i,j) < d_{\text{MST-path}(i,j)}^{\text{max}} + \gamma(d(i,i_k) + d(j,j_k)) \\ 0 & \text{otherwise} \end{cases}$$
 (7)

where  $\gamma$  is a positive density parameter. RMST includes the term  $\gamma(d(i,i_k)+d(j,j_k))$  in which  $\gamma d(i,i_k)$  and  $\gamma d(j,j_k)$  approximate the local distribution of samples around i and j, respectively [45]. In this work, we fix k=1 and vary different  $\gamma$  as suggested in [37].

#### **Graph sparsification**

The previous two types of methods (Neighborhood-based and MST-based) belong to the scope of graph densification in which the starting point is N samples and no edges exist between them. If the distance d(i,j) between two samples i and j meets a defined criteria, an edge is then established between them. The opposite scope of graph densification is graph sparsification where the starting point is usually a dense graph and the goal is to obtain a sparse graph which represents a good approximation of the given graph. The sparsified graph obtained through graph sparsification can be used in numerical computation without introducing too much error. Moreover, it is cheaper to deal with the sparsified graph for both numerical computation and data storage [41]. In this paper, we focus on spectral sparsification [41] of graphs which aims at obtaining a spectral approximation of the given graph. In particular, we apply the well-known Spielman-Srivastava sparsification algorithm (SSSA) proposed in [25] to sparsify optimal graphs constructed from the graph construction methods. The resulting graph satisfies the criteria below:

$$(1 - \epsilon)x^{\mathrm{T}} L x \le x^{\mathrm{T}} \widetilde{L} x \le (1 + \epsilon)x^{\mathrm{T}} L x \tag{8}$$

where L and  $\widetilde{L}$  are the Laplacian matrices of the given graph and resulting graph, respectively. The sparsification in SSSA is guided by a sparsity parameter  $(\sigma)$  which can range from 0 to 1.  $x \in R^{N \times 1}$  is a vector associated with nodes in the graph.

# **Graph Convolutional Networks**

Graph neural networks (GNNs), a new class of deep learning algorithms, have been recently proposed to address the graph-structured data. In particular, we focus on Graph Convolutional Networks (GCNs) [5] and their applications to semi-supervised setting. Each sample i is characterized by a F-dimensional feature vector  $X_i \in R^{1 \times F}$ , which is arranged into the feature matrix  $X \in R^{N \times F}$ . In addition, N samples are also associated with a graph  $\mathcal G$  where N samples are nodes and edges represent additional relational (symmetric) information. The graph is described by an adjacency matrix A. Each sample is also associated with one of F classes, which is encoded into a 0-1 membership matrix  $Y \in R^{N \times C}$ . GCN classification uses a small subset of ground truth labels, the full feature matrix, and the full graph to train a model, which is then used to predict the class of unlabeled nodes and evaluate the classification performance by comparing inferred labels with their ground truth labels.

Our study applies the two-layer GCN proposed in [5]. Given the feature matrix X and the (undirected) adjacency matrix A of the graph  $\mathcal{G}$ , the propagation rule is given by:

$$Z = f(X, A) = \operatorname{softmax}(\widehat{A} \operatorname{ReLU}(\widehat{A}XW^0) W^1), \tag{9}$$

where  $W^0$  and  $W^1$  are the weights connecting layers of the GCN. The graph is encoded in  $\widehat{A} = \widetilde{D}^{-1/2}(A+I_N)\widetilde{D}^{-1/2}$ , where  $I_N$  is the identity matrix, and  $\widetilde{D}$  is a diagonal matrix with  $\widetilde{D}_{ii} = 1 + \sum_j A_{ij}$ . The softmax and ReLU are threshold activation functions defined below:

$$ReLU(x)_i = \max(x_i, 0) \tag{10}$$

$$\operatorname{softmax}(x)_i = \frac{\exp(x_i)}{\sum_j \exp(x_j)}$$
(11)

where x is a vector.

In this semi-supervised multi-class classification, the cross-entropy error over all labeled samples is evaluated as follows:

$$\mathcal{L} = -\sum_{l \in \mathbb{Y}_L} \sum_{c=1}^C Y_{lc} \ln Z_{lc}, \tag{12}$$

where  $Y_L$  is the set of nodes that have labels (i.e., training set). The weights of the neural network ( $W^0$  and  $W^1$ ) are trained using gradient descent to minimize the loss  $\mathcal{L}$ .

## GCN architecture, hyperparameters and implementation

We use the GCN implementation provided by the authors of [5], and follow closely the experimental setup suggested in [5, 32]. We use a two-layer GCN as described before with 2,000 epochs (training iterations) and a learning rate of 0.01, and early stopping with a window size of 200. Other hyperparameters used are: i) dropout rate: 0.5; (ii) L2 regularization:  $5 \times 10^{-4}$ ; and (iii) number of hidden units: 16. The weights are initialized as described in [46], and the input feature vectors are accordingly L1 row-normalized. We choose the same data set splits as in [32] with 5% of samples as training set, 10% of samples as validation set and the remaining 85% as test set. The samples in the training set are evenly distributed across classes.

## **Baselines**

We consider four graph-less classification methods as baselines where no graph structure is explicitly used: GCN (No graph) which is equivalent to Multilayer Perceptron (MLP) [32], kNN Classification (kNNC), Support Vector Machine (SVM) and Random Forest (RF). We compare GCN with the optimized graph constructed against these baselines. The main baseline is GCN (No graph) [32], a limiting case of GCN, where the graph used in GCN is a graph with no edges, i.e.,  $A = \mathbf{00}^T$ , which is equivalent to an MLP. The classification is based solely on the information contained in the features since no graph structure is provided to guide the prorogation of features in the training. We further compare against kNNC. kNNC classifies the unseen samples based on the plurality vote of its neighbors. The sample in the test set will be assigned to the class which is the most common among its k-nearest neighbors in the training set. In particular, we apply an SVM with Radial Basis Function (RBF) kernel. We optimize the following hyperparameters based on the classification performance of validation set: number of neighbors in kNNC, regularization parameter in SVM and maximum depth in RF for each data set separately. We also perform L1 row-normalization on the original feature matrix for baselines.

#### Data and code availability

We provide the data sets and code for geometric graph construction at https://github.com/haczqyf/ggc. The sources for other related code (e.g., GCN and graph sparsification) are described in the SI Appendix.

# Acknowledgments

Yifan Qian acknowledges financial support from the China Scholarship Council program (No. 201706020176).

# References

- [1] Yann LeCun, Yoshua Bengio, and Geoffrey Hinton. Deep learning. Nature, 521(7553):436–444, 2015.
- [2] Michael M Bronstein, Joan Bruna, Yann LeCun, Arthur Szlam, and Pierre Vandergheynst. Geometric deep learning: going beyond euclidean data. *IEEE Signal Processing Magazine*, 34(4):18–42, 2017.
- [3] Danfei Xu, Yuke Zhu, Christopher B Choy, and Li Fei-Fei. Scene graph generation by iterative message passing. In *Proceedings of the IEEE Conference on Computer Vision and Pattern Recognition*, pages 5410–5419, 2017.
- [4] Loic Landrieu and Martin Simonovsky. Large-scale point cloud semantic segmentation with superpoint graphs. In *Proceedings of the IEEE Conference on Computer Vision and Pattern Recognition*, pages 4558–4567, 2018.
- [5] Thomas N. Kipf and Max Welling. Semi-supervised classification with graph convolutional networks. In *International Conference on Learning Representations (ICLR)*, 2017.
- [6] Will Hamilton, Zhitao Ying, and Jure Leskovec. Inductive representation learning on large graphs. In *Advances in Neural Information Processing Systems*, pages 1024–1034, 2017.
- [7] Petar Veličković, Guillem Cucurull, Arantxa Casanova, Adriana Romero, Pietro Liò, and Yoshua Bengio. Graph attention networks. In *International Conference on Learning Representations (ICLR)*, 2018.
- [8] Yaguang Li, Rose Yu, Cyrus Shahabi, and Yan Liu. Diffusion convolutional recurrent neural network: data-driven traffic forecasting. In *International Conference on Learning Representations (ICLR)*, 2018.
- [9] Bing Yu, Haoteng Yin, and Zhanxing Zhu. Spatio-temporal graph convolutional networks: A deep learning framework for traffic forecasting. In *Proceedings of the 27th International Joint Conference on Artificial Intelligence (IJCAI)*, 2018.
- [10] Rex Ying, Ruining He, Kaifeng Chen, Pong Eksombatchai, William L Hamilton, and Jure Leskovec. Graph convolutional neural networks for web-scale recommender systems. In *Proceedings of the 24th ACM SIGKDD International Conference on Knowledge Discovery & Data Mining*, pages 974–983, 2018.
- [11] Federico Monti, Michael Bronstein, and Xavier Bresson. Geometric matrix completion with recurrent multi-graph neural networks. In *Advances in Neural Information Processing Systems*, pages 3697–3707, 2017.
- [12] David K Duvenaud, Dougal Maclaurin, Jorge Iparraguirre, Rafael Bombarell, Timothy Hirzel, Alán Aspuru-Guzik, and Ryan P Adams. Convolutional networks on graphs for learning molecular fingerprints. In *Advances in Neural Information Processing Systems*, pages 2224–2232, 2015.
- [13] P Gainza, F Sverrisson, F Monti, E Rodolà, D Boscaini, MM Bronstein, and BE Correia. Deciphering interaction fingerprints from protein molecular surfaces using geometric deep learning. *Nature Methods*, 17(2):184–192, 2020.
- [14] Miltiadis Allamanis, Marc Brockschmidt, and Mahmoud Khademi. Learning to represent programs with graphs. In *International Conference on Learning Representations (ICLR)*, 2018.
- [15] Jiezhong Qiu, Jian Tang, Hao Ma, Yuxiao Dong, Kuansan Wang, and Jie Tang. Deepinf: Social influence prediction with deep learning. In *Proceedings of the 24th ACM SIGKDD International Conference on Knowledge Discovery & Data Mining*, pages 2110–2119, 2018.
- [16] Daniel Zügner, Amir Akbarnejad, and Stephan Günnemann. Adversarial attacks on neural networks for graph data. In Proceedings of the 24th ACM SIGKDD International Conference on Knowledge Discovery & Data Mining, pages 2847–2856, 2018.
- [17] Edward Choi, Mohammad Taha Bahadori, Le Song, Walter F Stewart, and Jimeng Sun. Gram: graph-based attention model for healthcare representation learning. In *Proceedings of the 23rd ACM SIGKDD International Conference on Knowledge Discovery and Data Mining*, pages 787–795, 2017.
- [18] Edward Choi, Cao Xiao, Walter Stewart, and Jimeng Sun. Mime: Multilevel medical embedding of electronic health records for predictive healthcare. In *Advances in Neural Information Processing Systems*, pages 4547–4557, 2018.
- [19] Zhuwen Li, Qifeng Chen, and Vladlen Koltun. Combinatorial optimization with graph convolutional networks and guided tree search. In *Advances in Neural Information Processing Systems*, pages 539–548, 2018.
- [20] Zonghan Wu, Shirui Pan, Fengwen Chen, Guodong Long, Chengqi Zhang, and S Yu Philip. A comprehensive survey on graph neural networks. *IEEE Transactions on Neural Networks and Learning Systems*, 2020.
- [21] Andrew Zalesky, Alex Fornito, and Edward T Bullmore. On the use of correlation as a measure of network connectivity. *NeuroImage*, 60(4):2096–2106, May 2012.

- [22] Louis-David Lord, Paul Allen, Paul Expert, Oliver Howes, Matthew Broome, Renaud Lambiotte, Paolo Fusar-Poli, Isabel Valli, Philip McGuire, and Federico E Turkheimer. Functional brain networks before the onset of psychosis: A prospective fMRI study with graph theoretical analysis. *NeuroImage. Clinical*, 1(1):91–98, 2012.
- [23] Nooshin Omranian, Jeanne M O Eloundou-Mbebi, Bernd Mueller-Roeber, and Zoran Nikoloski. Gene regulatory network inference using fused LASSO on multiple data sets. *Scientific Reports*, 6(1):20533, February 2016.
- [24] Tyrus Berry and Timothy Sauer. Consistent manifold representation for topological data analysis. *Foundations of Data Science*, 1(1):1–38, 2019.
- [25] Daniel A Spielman and Nikhil Srivastava. Graph sparsification by effective resistances. *SIAM Journal on Computing*, 40(6):1913–1926, 2011.
- [26] Mariano Beguerisse-Díaz, Borislav Vangelov, and Mauricio Barahona. Finding role communities in directed networks using role-based similarity, markov stability and the relaxed minimum spanning tree. In 2013 IEEE Global Conference on Signal and Information Processing, pages 937–940. IEEE, 2013.
- [27] Yifan Qian, Wenge Rong, Nan Jiang, Jie Tang, and Zhang Xiong. Citation regression analysis of computer science publications in different ranking categories and subfields. *Scientometrics*, 110(3):1351–1374, 2017.
- [28] Jie Tang, Jing Zhang, Limin Yao, Juanzi Li, Li Zhang, and Zhong Su. Arnetminer: extraction and mining of academic social networks. In *Proceedings of the 14th ACM SIGKDD international conference on Knowledge discovery and data mining*, pages 990–998, 2008.
- [29] Luca Franceschi, Mathias Niepert, Massimiliano Pontil, and Xiao He. Learning discrete structures for graph neural networks. In *Proceedings of the 36th International Conference on Machine Learning*, 2019.
- [30] Michaël Defferrard, Kirell Benzi, Pierre Vandergheynst, and Xavier Bresson. Fma: A dataset for music analysis. *arXiv preprint arXiv:1612.01840*, 2016.
- [31] Dmitry Velmeshev, Lucas Schirmer, Diane Jung, Maximilian Haeussler, Yonatan Perez, Simone Mayer, Aparna Bhaduri, Nitasha Goyal, David H Rowitch, and Arnold R Kriegstein. Single-cell genomics identifies cell type–specific molecular changes in autism. *Science*, 364(6441):685–689, 2019.
- [32] Yifan Qian, Paul Expert, Tom Rieu, Pietro Panzarasa, and Mauricio Barahona. Quantifying the alignment of graph and features in deep learning. arXiv preprint arXiv:1905.12921, 2019.
- [33] Ake Björck and Gene H Golub. Numerical methods for computing angles between linear subspaces. *Mathematics of Computation*, 27(123):579–594, 1973.
- [34] Gene H Golub and Charles F Van Loan. Matrix computations, volume 3. JHU press, 2012.
- [35] Andrew V Knyazev and Merico E Argentati. Principal angles between subspaces in an a-based scalar product: algorithms and perturbation estimates. *SIAM Journal on Scientific Computing*, 23(6):2008–2040, 2002.
- [36] Laurens van der Maaten and Geoffrey Hinton. Visualizing data using t-sne. *Journal of Machine Learning Research*, 9(Nov):2579–2605, 2008.
- [37] Zijing Liu and Mauricio Barahona. Graph-based data clustering via multiscale community detection. *Applied Network Science*, 5(1):3, 2020.
- [38] Qimai Li, Zhichao Han, and Xiao-Ming Wu. Deeper insights into graph convolutional networks for semi-supervised learning. In *Thirty-Second AAAI Conference on Artificial Intelligence*, 2018.
- [39] Deli Chen, Yankai Lin, Wei Li, Peng Li, Jie Zhou, and Xu Sun. Measuring and relieving the over-smoothing problem for graph neural networks from the topological view. In *Thirty-Fourth AAAI Conference on Artificial Intelligence*, 2020.
- [40] Renaud Lambiotte, Jean-Charles Delvenne, and Mauricio Barahona. Random walks, markov processes and the multiscale modular organization of complex networks. *IEEE Transactions on Network Science and Engineering*, 1(2):76–90, 2014.
- [41] Daniel A Spielman and Shang-Hua Teng. Spectral sparsification of graphs. *SIAM Journal on Computing*, 40(4):981–1025, 2011.
- [42] Wai-Shing Fung, Ramesh Hariharan, Nicholas JA Harvey, and Debmalya Panigrahi. A general framework for graph sparsification. *SIAM Journal on Computing*, 48(4):1196–1223, 2019.
- [43] Miloš Radovanović, Alexandros Nanopoulos, and Mirjana Ivanović. Hubs in space: Popular nearest neighbors in high-dimensional data. *Journal of Machine Learning Research*, 11(Sep):2487–2531, 2010.
- [44] Kohei Ozaki, Masashi Shimbo, Mamoru Komachi, and Yuji Matsumoto. Using the mutual k-nearest neighbor graphs for semi-supervised classification of natural language data. In *Proceedings of the Fifteenth Conference on Computational Natural Language Learning*, pages 154–162, 2011.

- [45] Richard S Zemel and Miguel Á Carreira-Perpiñán. Proximity graphs for clustering and manifold learning. In *Advances in Neural Information Processing Systems*, pages 225–232, 2005.
- [46] Xavier Glorot and Yoshua Bengio. Understanding the difficulty of training deep feedforward neural networks. In *Proceedings of the Thirteenth International Conference on Artificial Intelligence and Statistics*, pages 249–256, 2010.
- [47] Prithviraj Sen, Galileo Namata, Mustafa Bilgic, Lise Getoor, Brian Galligher, and Tina Eliassi-Rad. Collective classification in network data. *AI Magazine*, 29(3):93–93, 2008.
- [48] Fabian Pedregosa, Gaël Varoquaux, Alexandre Gramfort, Vincent Michel, Bertrand Thirion, Olivier Grisel, Mathieu Blondel, Peter Prettenhofer, Ron Weiss, Vincent Dubourg, et al. Scikit-learn: Machine learning in python. *Journal of Machine Learning Research*, 12(Oct):2825–2830, 2011.
- [49] Nathanaël Perraudin, Johan Paratte, David Shuman, Lionel Martin, Vassilis Kalofolias, Pierre Vandergheynst, and David K Hammond. Gspbox: A toolbox for signal processing on graphs. *arXiv preprint arXiv:1408.5781*, 2014.

# **Supplementary information**

#### A Data sets

We use seven data sets collected from various sources. We provide the data sets at https://github.com/haczqyf/ggc/tree/master/ggc/data. The data set statistics are summarized in Table 1.

- 1. Constructive [32] is a synthetic data set generated by a stochastic block model that reproduces the ground truth structure with some noise. Each ground truth cluster is associated with 50 features with a probability of  $p_{\rm in}=0.07$  equal to 1. Each sample also has a probability of  $p_{\rm out}=0.007$  of possessing each feature characterizing other clusters.
- 2. We consider two data sets with text documents: *Cora* [47, 32] and *AMiner* [27, 28]. In Cora and AMiner, the samples are scientific papers where each paper is associated with a high-dimensional bag-of-words feature vector extracted from the paper content. Each sample has a class label indicating its scientific field.
- 3. *Digits* is a handwritten digits data set. Each sample is a 8x8 image of a digit. This is one of the benchmark data sets for classification in Scikit-learn [48].
- 4. *FMA*: The original data set [29, 30] contains 140 audio features extracted from 7,994 music tracks and where the problem is genre classification. The original data set in [29] contains 8 genres. We sample randomly 2,000 music tracks (250 for each genre) to produce our data set.
- 5. Cell: This is a brain cell types from autism dataset. The original data set [31] contains the gene expression values ( $\log_2$  transformed 10x UMI counts from cellranger) of 104,599 single cells from brains of control individuals and of patients with autism, where each cell (sample) is characterized by the expression level of 36,501 genes (features). The full data set contains cells from 17 cell types (categories). To produce our data set, we sample randomly 2,000 cells from 10 cell types (200 cells for each type) and select as our features the expression level of the top 500 most highly variable genes across the 2,000 cells in our sample.
- 6. Segmentation: This is an image segmentation data set, which is provided at UCI machine learning repository at http://archive.ics.uci.edu/ml/datasets/image+segmentation. Each sample represents an image described by 19 high-level and man-crafted numeric-valued attributes.

# **B** Code availability

We provide the data sets and code for geometric graph construction at https://github.com/haczqyf/ggc. The code for Graph Convolutional Networks (GCN) is provided by the authors of [5] at https://github.com/tkipf/gcn. The code for kNN Classification (kNNC), Support Vector Machine (SVM) and Random Forest (RF) can be found at https://scikit-learn.org/stable/ from scikit-learn [48]. The code for Spielman-Srivastava sparsification algorithm (SSSA) is available at https://epf1-lts2.github.io/gspbox-html/doc/utils/gsp\_graph\_sparsify.html from Graph Signal Processing Toolbox [49].

# C Tables and Figures

Table 1: Summary statistics of the data sets in our study.

Data sets	Туре	Samples (N)	Features (F)	Classes (C)	Train/Validation/Test
Constructive	Stochastic block model	1,000	500	10	50/100/850
Cora	Text (Bag-of-words)	2,485	1,433	7	119/253/2,113
AMiner	Text (Bag-of-words)	2,072	500	7	98/212/1,762
Digits	Images (Grayscale pixels)	1,797	64	10	80/189/1,528
FMA (songs)	Music track features	2,000	140	8	96/204/1,700
Brain cell types	Single-cell transcriptomics	2,000	500	10	100/200/1,700
Segmentation	Image features	2310	19	7	112/234/1,964

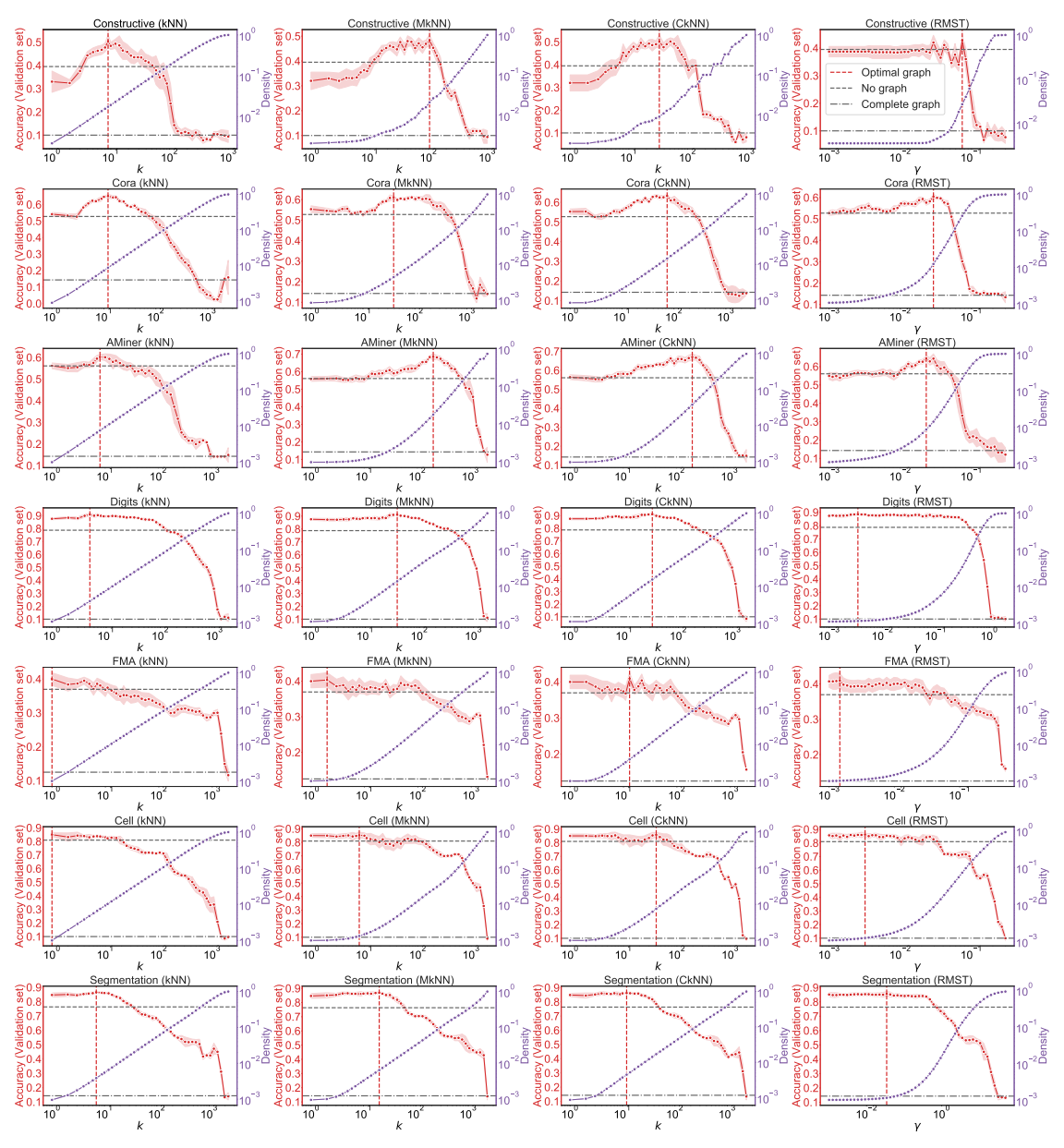


Figure 4: The red line indicates the mean classification accuracy on the validation set of 10 runs with random weight initializations as a function of the density parameter. The red shaded regions denote the standard deviation. The mean classification accuracy on the validation of two limiting cases (no graph and complete graph) are added as well. The red vertical line indicates the optimal graph. The purple line shows the densities of the constructed CkNN graphs.

Table 2: Selected density parameters and density of constructed graphs in the graph densification process (Fig. 4)

	kNN		MkNN		$\mathbf{CkNN}  (\delta = 1)$		$\mathbf{RMST} (k=1)$	
Data set	$k^*$	Density	$k^*$	Density	$k^*$	Density	$\gamma^*$	Density
Constructive	9	0.01741	104	0.02101	33	0.00920	0.07421	0.02724
Cora	12	0.00842	39	0.00436	74	0.01476	0.02924	0.01242
AMiner	8	0.00748	199	0.01786	199	0.03852	0.02317	0.00859
Digits	5	0.00404	39	0.01400	33	0.01564	0.00346	0.00117
FMA	1	0.00100	2	0.00103	13	0.00398	0.00146	0.00107
Cell	1	0.00100	8	0.00133	41	0.00753	0.00320	0.00124
Segmentation	7	0.00387	20	0.00637	12	0.00447	0.03423	0.00117

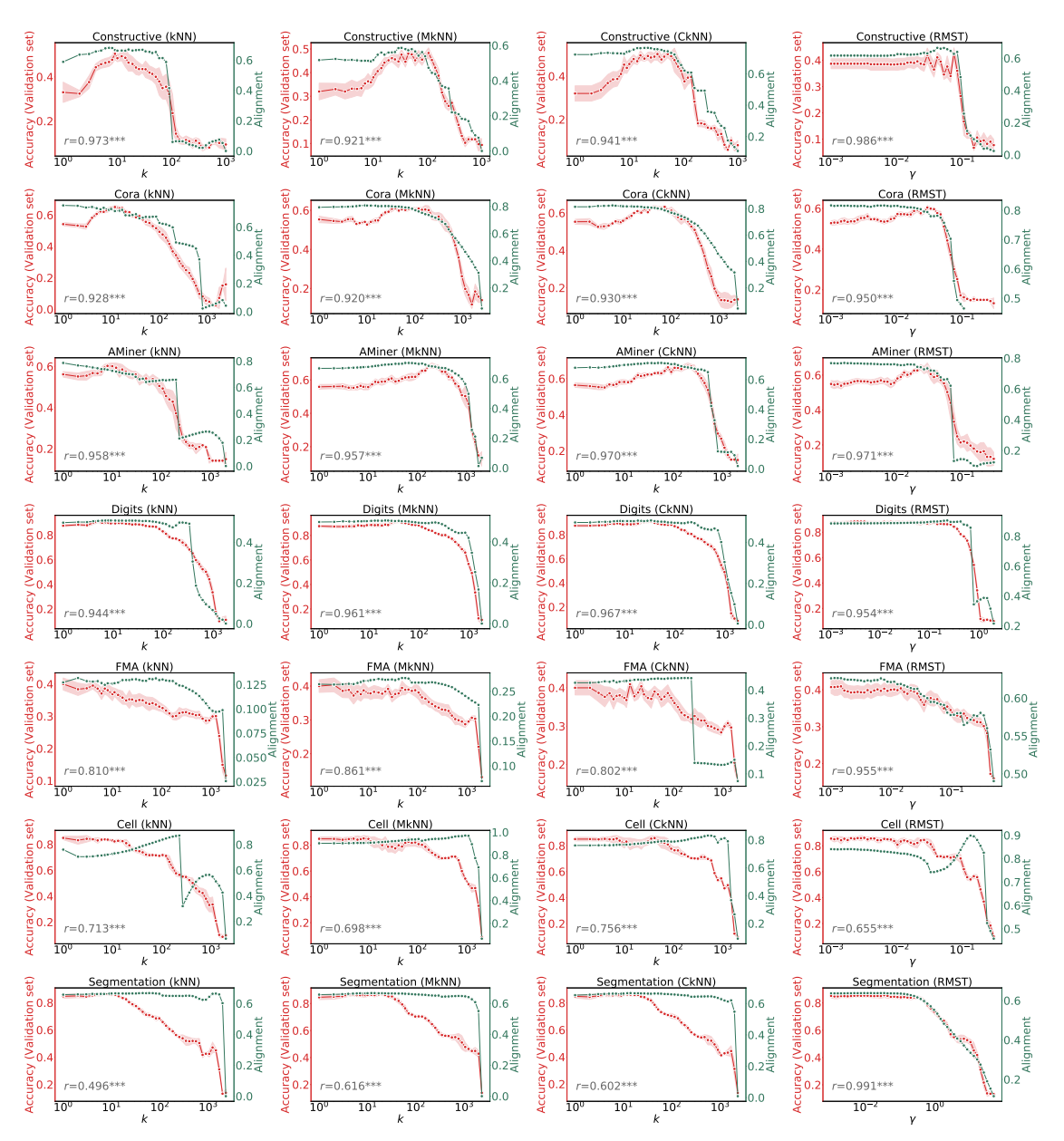


Figure 5: The red line indicates the mean classification accuracy on the validation set of 10 runs with random weight initializations as a function of the density parameter k in CkNN. The red shaded regions denote the standard deviation. The green line indicates the alignment. We report the Pearson correlation coefficients and p-values between mean accuracy and alignment. \*p-value < 0.05,\*\* p-value < 0.01,\*\*\* p-value < 0.001.

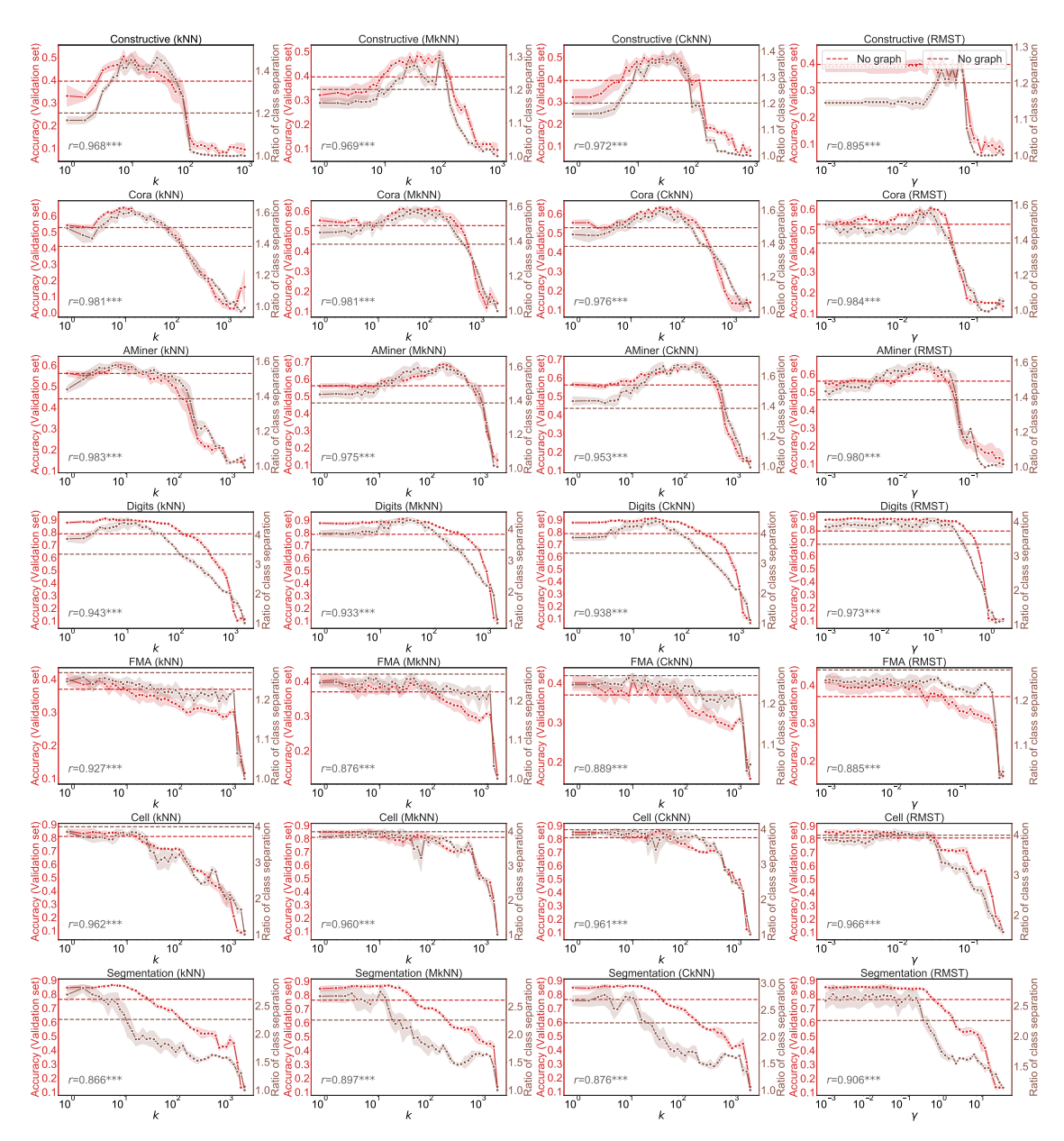


Figure 6: The red line indicates the mean classification accuracy on the validation set of 10 runs with random weight initializations as a function of the density parameter k in CkNN. The red shaded regions denote the standard deviation. The red dashed line represents the mean classification accuracy on the validation of no graph case. The brown line shows the ratio of class separation in the densification process. The brown shaded regions denote the standard deviation. The brown dashed line represents the ratio of class separation of no graph case. We report the Pearson correlation coefficients and p-values between mean accuracy and mean ratio of class separation. \*p-value < 0.05,\*\* p-value < 0.01,\*\*\* p-value < 0.001.

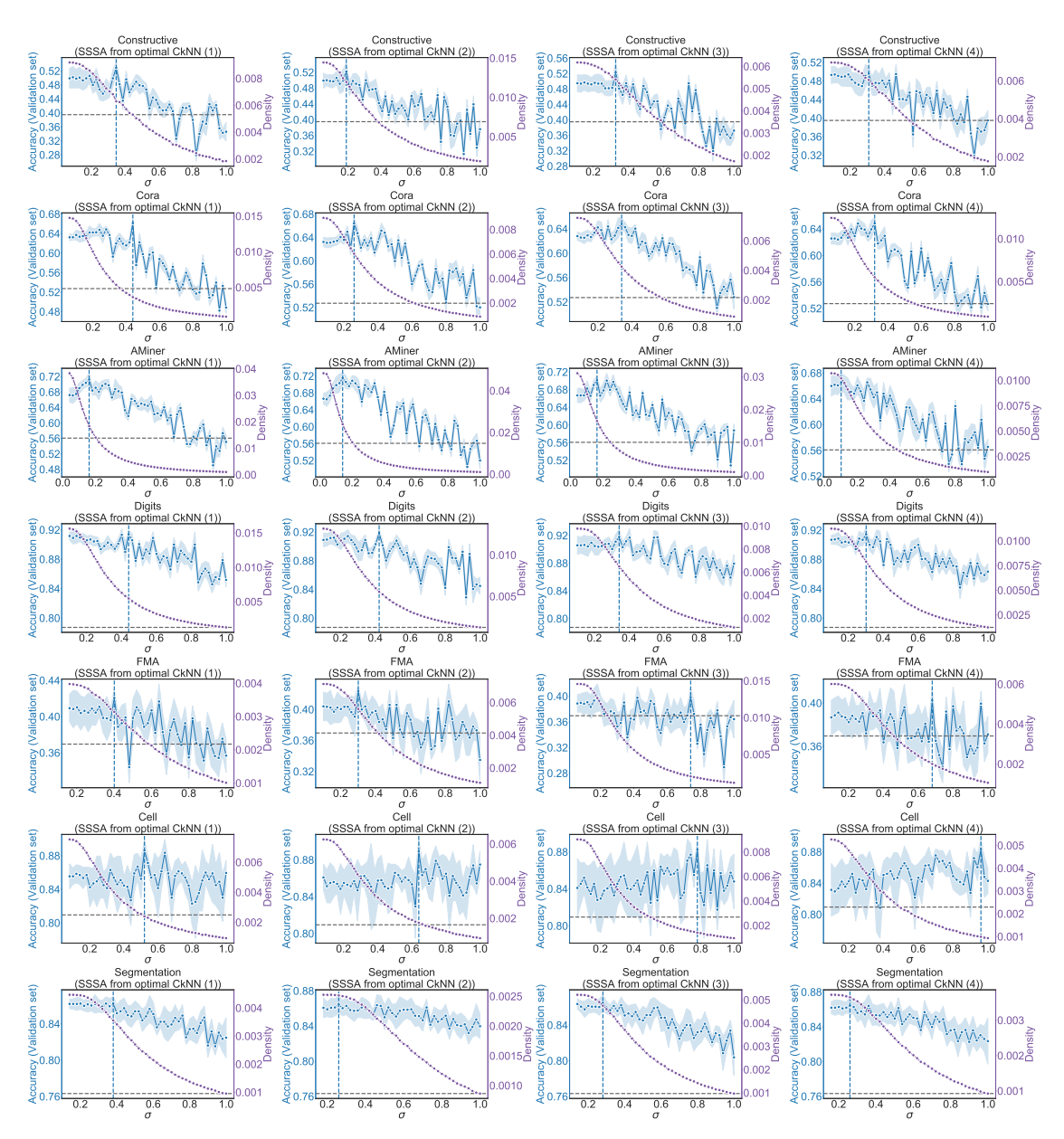


Figure 7: The blue line indicates the mean classification accuracy on the validation set of 10 runs with random weight initializations as a function of the sparsity parameter. The blue shaded regions denote the standard deviation. The mean classification accuracy on the validation of no graph is added as well. The blue vertical line indicates the optimal graph on the validation set. The purple line shows the densities of the sparsified graphs.

Table 3: Comparison between optimal graphs and sparsified graphs (Fig. 7).

Top 4 CkNN graphs			Optimal CkNN Sparsified CkNN							
on validation set	Data set	$k^*$	Edge density	$\langle k \rangle$	Accuracy (Test)	$\sigma^*$	Edge density	$\langle k \rangle$	Accuracy (Test)	
	Constructive	33	0.00920	9.2	51.1	0.3479	0.00630	6.3	51.6	
	Cora	74	0.01476	36.7	66.6	0	0.01476	36.7	66.6	
	AMiner	199	0.03852	79.8	61.6	0.1618	0.01840	38.1	62.5	
(1)	Digits	33	0.01564	28.1	93.4	0	0.01564	28.1	93.4	
	FMA	13	0.00398	8.0	36.0	0	0.00398	8.0	36.0	
	Cell	41	0.00753	15.0	84.0	0.5212	0.00240	4.8	85.0	
	Segmentation	12	0.00447	10.3	83.9	0.3806	0.00356	8.2	84.0	
	Average improvement			(+8.3)				(+8.7)		
	Constructive	51	0.01445	14.4	51.8	0.1898	0.01197	12.0	53.6	
	Cora	46	0.00897	22.3	66.3	0	0.00897	22.3	66.3	
	AMiner	233	0.04838	100.2	61.3	0.1418	0.02396	49.6	63.6	
(2)	Digits	28	0.01319	23.7	93.2	0.4222	0.00556	10.0	93.2	
	FMA	22	0.00713	14.3	35.2	0.3018	0.00561	11.2	35.8	
	Cell	35	0.00625	12.5	83.6	0.6409	0.00176	3.5	86.9	
	Segmentation	7	0.00253	5.8	84.0	0.2607	0.00252	5.8	84.2	
	Average improvement				(+8.1)				(+9.3)	
	Constructive	16	0.00618	6.2	49.0	0	0.00618	6.2	49.0	
	Cora	39	0.00756	18.8	66.8	0	0.00756	18.8	66.8	
(3)	AMiner	171	0.03115	64.5	62.1	0.1618	0.01656	34.3	63.5	
	Digits	21	0.00978	17.6	92.9	0.3425	0.00650	11.7	93.0	
	FMA	41	0.01457	29.1	35.9	0	0.01457	29.1	35.9	
	Cell	48	0.00904	18.1	81.9	0.7806	0.00141	2.8	84.1	
	Segmentation	14	0.00522	12.1	83.8	0	0.00522	12.1	83.8	
	Average improvement				(+7.7)				(+8.2)	
	Constructive	22	0.00697	7.0	51.2	0.3084	0.00605	6.0	51.4	
	Cora	63	0.01246	30.9	65.9	0	0.01246	30.9	65.9	
	AMiner	78	0.01071	22.2	62.0	0.1019	0.01021	21.1	62.1	
(4)	Digits	24	0.01125	20.2	92.9	0	0.01125	20.2	92.9	
	FMA	19	0.00601	12.0	34.5	0.6808	0.00201	4.0	35.2	
	Cell	30	0.00527	10.5	81.8	0.9601	0.00099	2.0	85.3	
	Segmentation	10	0.00372	8.6	83.9	0.2607	0.00365	8.4	84.1	
	Average improvement				(+7.7)				(+8.3)	

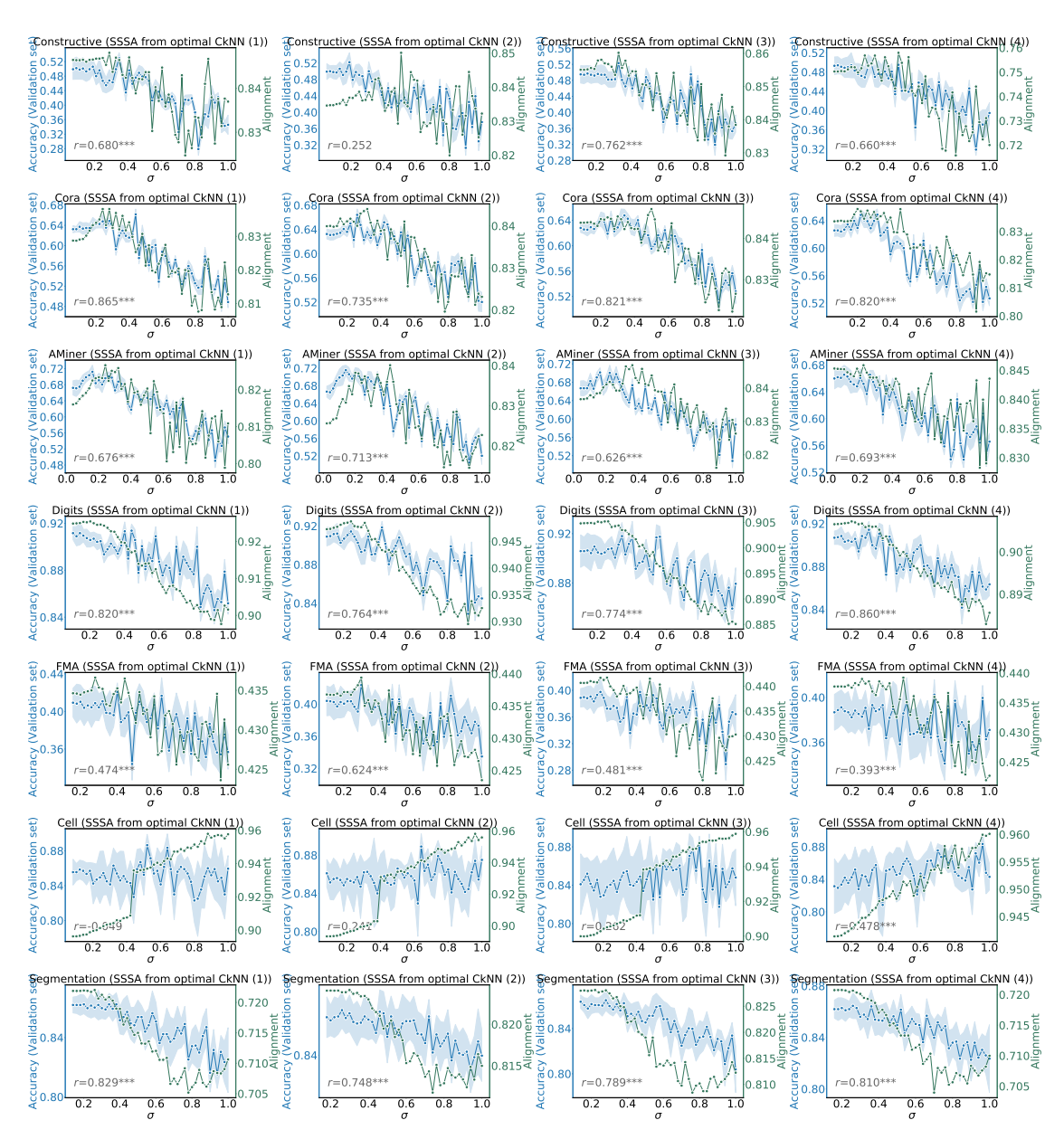


Figure 8: The blue line indicates the mean classification accuracy on the validation set of 10 runs with random weight initializations as a function of the sparsity parameter. The blue shaded regions denote the standard deviation. The green line indicates the alignment. We report the Pearson correlation coefficients and p-values between mean accuracy and alignment. \*p-value < 0.05,\*\* p-value < 0.01,\*\*\* p-value < 0.001.

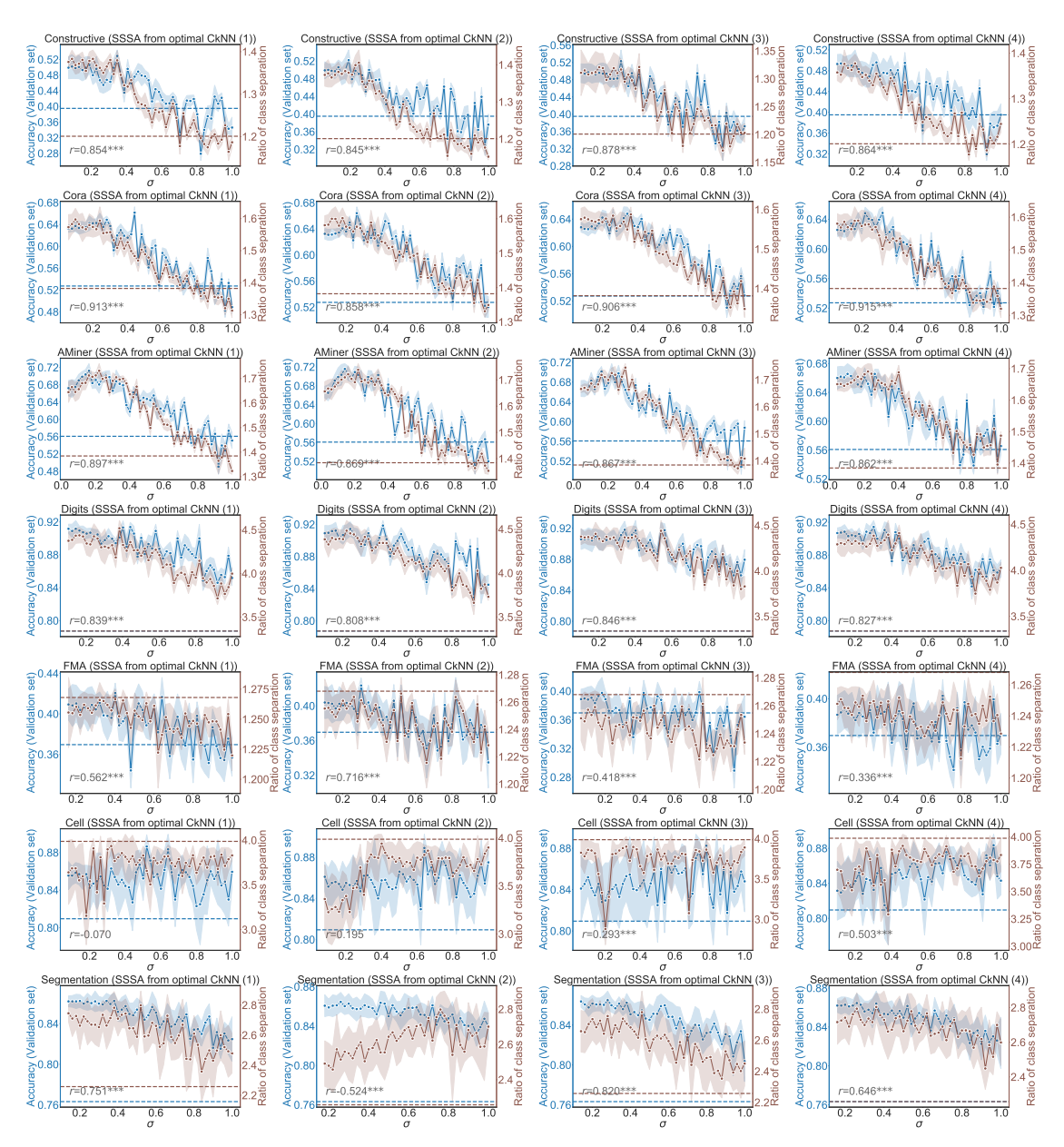


Figure 9: The blue line indicates the mean classification accuracy on the validation set of 10 runs with random weight initializations as a function of the sparsity parameter. The blue shaded regions denote the standard deviation. The blue dashed line represents the mean classification accuracy on the validation of no graph case. The brown line shows the ratio of class separation in the densification process. The brown shaded regions denote the standard deviation. The brown dashed line represents the ratio of class separation of no graph case. We report the Pearson correlation coefficients and p-values between mean accuracy and mean ratio of class separation. \*p-value < 0.05,\*\* p-value < 0.01,\*\*\* p-value < 0.001.